


Downscaling future climate change projections over Puerto Rico using a non-hydrostatic atmospheric model

Amit Bhardwaj^{1,2}  • Vasubandhu Misra^{1,2,3} •
Akhilesh Mishra^{1,4} • Adrienne Wootten⁵ •
Ryan Boyles⁵ • J. H. Bowden⁶ • Adam J. Terando^{7,8}

Received: 30 March 2016 / Accepted: 23 December 2017
© Springer Science+Business Media B.V., part of Springer Nature 2018

Abstract We present results from 20-year “high-resolution” regional climate model simulations of precipitation change for the sub-tropical island of Puerto Rico. The Japanese Meteorological Agency Non-Hydrostatic Model (NHM) operating at a 2-km grid resolution is nested inside the Regional Spectral Model (RSM) at 10-km grid resolution, which in turn is forced at the lateral boundaries by the Community Climate System Model (CCSM4). At this resolution, the climate change experiment allows for deep convection in model integrations, which is an important consideration for sub-tropical regions in general, and on islands with steep precipitation gradients in particular that strongly influence local ecological processes and the provision of ecosystem services. Projected precipitation change for this region of the Caribbean is simulated for the mid-twenty-first century (2041–2060) under the RCP8.5 climate-forcing scenario relative to the late twentieth century (1986–2005). The results show that by the mid-twenty-first century, there is an overall rainfall reduction over the island for all seasons compared to the recent climate

Electronic supplementary material The online version of this article (<https://doi.org/10.1007/s10584-017-2130-x>) contains supplementary material, which is available to authorized users.

✉ Amit Bhardwaj
abhardwaj@coaps.fsu.edu

¹ Center for Ocean-Atmospheric Prediction Studies, Florida State University, Tallahassee, FL, USA

² Florida Climate Institute, Florida State University, Tallahassee, FL, USA

³ Department of Earth, Ocean and Atmospheric Science, Florida State University, Tallahassee, FL, USA

⁴ Center for Ocean-Atmospheric Science and Technology (COAST), Amity University Rajasthan, Jaipur, India

⁵ Department of Marine, Earth, and Atmospheric Sciences, North Carolina State University, Raleigh, NC, USA

⁶ Institute of the Environment, University of North Carolina at Chapel Hill, Chapel Hill, NC, USA

⁷ U.S. Geological Survey, Southeast Climate Science Center, Raleigh, NC, USA

⁸ Department of Applied Ecology, North Carolina State University, Raleigh, NC, USA

but with diminished mid-summer drought (MSD) in the northwestern parts of the island. Importantly, extreme rainfall events on sub-daily and daily time scales also become slightly less frequent in the projected mid-twenty-first-century climate over most regions of the island.

1 Introduction

Puerto Rico, a $\sim 9000\text{-km}^2$ island located within the Greater Antilles of the Caribbean, experiences a significant precipitation gradient. Precipitation amounts across the island can range from an average of 4346 mm year^{-1} in the northeast rainforest to less than 745 mm year^{-1} in the southwest. This gradient is largely the result of the two mountain systems on the island: the Cordillera Central that cuts across the center of the island in an approximately east-west orientation and the Sierra de Luquillo at 1065-m elevation in the northeast part of the island. Because the Luquillo Mountains are in a region subject to the moist Atlantic trade winds, they receive nearly twice the annual rainfall compared to that seen in the Central Mountains at an equivalent elevation (Waide et al. 2013). In addition, as a result of the impingement of the prevailing northeasterly trade winds on the Cordillera Central, confluent boundary layer circulations generate organized convective clouds on the lee side during the afternoon, particularly in the summer months (Jury and Chiao 2013). Similarly, the temperature declines with elevation from an annual average of $26.5\text{ }^\circ\text{C}$ at sea level near the coast to $20\text{ }^\circ\text{C}$ at the top of the Luquillo Mountains (Gonzalez and Luce 2013).

Prior downscaling efforts in this region either operated at resolutions that did not permit an explicit representation of convection (Campbell et al. 2011) or used statistical downscaling (Hayhoe 2013; Henareh et al. 2016) that operate under a strong stationarity assumption. We present in this paper the results of a 40-year simulation of the twentieth- and twenty-first-century climate over Puerto Rico from a nested 2-km Japanese Meteorological Agency Non-Hydrostatic Model (NHM; Saito et al. 2006). The NHM is nested in another regional model, the hydrostatic Regional Spectral Model (RSM; Kanamitsu et al. 2010) operating at 10-km grid resolution (see Table ST1). The RSM is in turn forced at the lateral boundaries by one of the Coupled Model Intercomparison Project version 5 (CMIP5; Taylor et al. 2012) models, the Community Climate System Model version 4 (CCSM4; Gent et al. 2011). The relatively small-scale orographic features and the size of the island warrant such high-resolution downscaling, as the coarser CMIP5 models typically in the range of $\sim 150\text{-km}$ grid resolution are barely able to resolve the island. Cantet et al. (2014) show that downscaling to higher resolutions in the Caribbean resolve some of the islands as land points, which is otherwise an open ocean point in the coarser global climate models (GCMs). This affects the projections of the future climate as physical processes for climate change over land are different from that over the open ocean. Further, this study and Chan et al. (2011) clearly indicate that the varying sizes of these Caribbean islands and the orography therein manifest in local climates that differ from one island to the other.

In recent years, with the advent of additional computational power, climate change studies at “convection-permitting”¹ resolutions have become possible (Kendon et al. 2014; Fosser et al. 2015). These models explicitly represent deep convection and avoid the use of convective parameterization schemes, which is thought to be the source of significant model errors

¹ They are termed convective permitting because at resolutions of order of 1-km grid spacing they are still unable to resolve convective plumes.

(Palmer 2001). Furthermore, there is a growing interest in understanding the behavior of precipitation extremes at daily (Min et al. 2011; Wuebbles et al. 2014) and sub-daily (Borga et al. 2011; Kendon et al. 2014) scales that are often the primary cause of flash flood events, especially with those related to convective type precipitation (Lenderink and van Meijgaard 2008; Haerter and Berg 2009).

Comarazamy and Gonzalez (2011) conducted a pseudo-global warming experiment using a nested high-resolution (5 km) regional climate model simulations and found significant relationships between global warming and the observed reduction of rainfall over the northeastern region of Puerto Rico. Similarly, Hayhoe (2013) used a statistical technique to downscale GCM projections and showed an overall reduction of precipitation over Puerto Rico from present climate under extreme greenhouse gas emission scenarios. Alternatively, in this study, we dynamically downscaled current and future projections of climate over the island of Puerto Rico to an unprecedented 2-km grid spacing and describe the impact of this model configuration on the fidelity of the simulation of precipitation and the projected changes under the RCP8.5 emission scenario (see Sect. S1), respectively.

2 Model setup and data

The twentieth-century historical simulation and the corresponding RCP8.5 emission scenario of the CCSM4 integrations were dynamically downscaled for the current (1986–2005) and future mid-century (2041–2060) climate over Puerto Rico. The single RCP8.5 emission scenario was chosen not only because of constraints on computation resources but also because the latest global CO₂ emissions continue to track the high end of this emission scenario (Peters et al. 2013). As such, RCP8.5 is a valuable scenario for gauging the potential risks associated with continuing our current (and increasing) rate of fossil fuel combustion. A brief outline of the model setups for downscaling is indicated in Table ST1 and illustrated in Fig. 1a. Here, we illustrate the results of dynamically downscaling a single GCM realization from CCSM4 to investigate projections of mean and extreme precipitation. The atmospheric grid resolution of the CCSM4 integration was $1.25^{\circ} \times 0.9^{\circ}$. This data was downscaled to 2-km grid spacing centered over the island of Puerto Rico using two, one-way nested regional atmospheric models. For the outer domain, we used the RSM at 10-km grid spacing forced by CCSM4 at the lateral boundaries. Amongst the CMIP5 models, the choice of CCSM4 was driven primarily by a desire to use a GCM that fairly captured the regional seasonal cycle of precipitation (Ryu and Hayhoe 2013). Further, dominant natural variations like El Niño and the Southern Oscillation (ENSO) in the CCSM4 twentieth-century simulation show improved fidelity compared to other CMIP5 models (Bellenger et al. 2014). In addition, the equilibrium climate sensitivity (defined as the equilibrium change in global mean surface air temperature to doubling of concentration of CO₂) is 3.2°C (Bitz et al. 2012). This is nearly in the middle of the range of $2.1\text{--}4.7^{\circ}\text{C}$ displayed by the suite of CMIP5 models (Andrews et al. 2012). Therefore, we chose CCSM4 to downscale, given this wide range of climate sensitivity and the limitation of resources to conduct the downscaling of one CMIP5 model. Lastly, the necessary fields for forcing the nested regional climate models for the historical period and all future emission scenarios under CMIP5 protocol were available for CCSM4, which makes it convenient to extend this study to other emission scenarios in future work.

The NHM (Saito et al. 2006) at 2-km grid interval was nested within the RSM (see Fig. 1a and Table ST1). There are 201×100 grid points in the RSM domain and 250×100 grid points

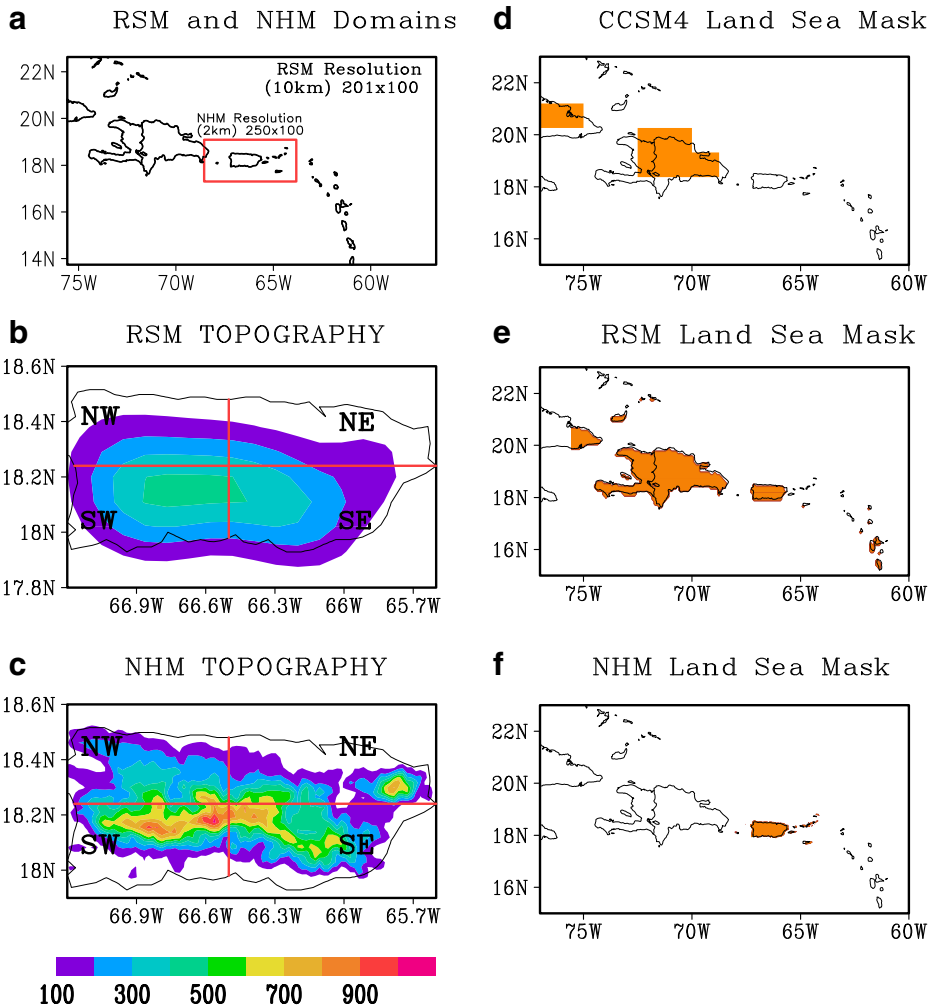


Fig. 1 **a** The outer domain represents the domain of the Regional Spectral Model (RSM) at 10-km grid resolution within which outlined in red is the domain of the Non-Hydrostatic Model (NHM) at 2-km grid resolution. The height of orography (meters) of Puerto Rico as resolved by **b** RSM at 10-km grid spacing and **c** NHM at 2-km grid spacing. The boundaries of the northwest (NW), northeast (NE), southwest (SW), and southeast (SE) parts of the island are marked by the bold line cutting across the island. Land (marked in orange) sea mask of **d** CCSM4, **e** RSM, and **f** NHM. The land-sea mask at each of the given resolution of the model provide a perspective on the spatial resolution of the models

in the NHM domain. Both the RSM and the NHM integrations for the current and the future climate were forced with the corresponding SSTs from the late twentieth-century historical and mid-twenty-first-century periods (under RCP8.5 emission scenario) of the CCSM4 centennial integrations, respectively. In both RSM and NHM future climate integrations, the greenhouse gas forcing was changed in accordance with the RCP8.5 emission scenario commensurate with an overall climate forcing of 8.5 W m^{-2} by the end of the twenty-first century (Riahi et al. 2011). This study over Puerto Rico is also unique from the perspective of using an RCP emission scenario as opposed to the SRES emission scenario of earlier downscaling studies

(Campbell et al. 2011; Hall et al. 2013; see Sect. S1). It is important to note that this downscaling experiment is the first result from a larger project to dynamically downscale multiple GCMs with a combination of regional climate models to further understand the uncertainty of the climate change projections at regional to local scales (e.g., Hawkins and Sutton 2009; Wootten et al. 2016).

The contrast of the spatial resolution of RSM and NHM for Puerto Rico is very apparent in the resolved topography (Fig. 1b and c) and the resolution of the islands itself (Fig. 1d, e, and f). In Fig. 1c, the Cordillera Central through the center of the island and Sierra de Luquillo in the northeast part of the island are clearly resolved in the NHM. In contrast, the Cordillera Central mountain range is much shallower and broader in the RSM (Fig. 1b). Furthermore, the Sierra de Luquillo in northeast Puerto Rico is not resolved at all in the RSM (Fig. 1b). The land-sea mask shown in Fig. 1d shows that the CCSM4 model leaves Puerto Rico completely unresolved, while the island appears in both the RSM (Fig. 1e) and NHM (Fig. 1f) model domains.

The RSM has an attractive feature of scale selective bias correction (SSBC) that allows the downscaling ratio to be much greater than typically used in other regional models (Kanamaru and Kanamitsu 2007). In the present study, SSBC constrains the RSM solution to the large-scale field of CCSM4 instead of atmospheric reanalysis as it was originally proposed for (Kanamaru and Kanamitsu 2007). Therefore, in a strict sense, SSBC is not a bias correction. However, it is necessary to implement this scheme to avoid large-scale drift of the regional climate model independent of the large-scale forcing (Von Storch et al., 2000; Misra 2006; Bowden et al. 2012, 2013) and avoid the results of RSM being critically dependent on the choice of the domain (Kanamaru and Kanamitsu 2007). We downscaled from the CCSM4 nominal 1° grid interval to the intermediate 10-km grid spacing of the RSM. This saved significant computing time and resources by avoiding multiple nesting to the 10-km grid resolution of RSM from the $1.25^\circ \times 0.9^\circ$ resolution of the CCMS4. The RSM has been routinely used at 10-km grid intervals in this manner in prior studies (Misra et al. 2012; Stefanova et al. 2012; DiNapoli and Misra 2012). A brief description of the RSM is presented in Table S2.

The NHM (Saito et al. 2006) is a grid point model that uses an Arakawa C-grid structure in the horizontal and a Lorenz type in the vertical (Saito et al. 2001). A fourth-order advection scheme on this staggered grid is implemented. A modified version of the leap frog scheme is used for time integration. Rayleigh damping sponge layers are imposed in the lateral boundaries of the NHM for momentum, pressure, potential temperature, and specific humidity. As part of the package of physical processes, NHM includes an explicit three-ice bulk micro-physics scheme (Ikawa and Saito 1991), atmospheric radiation based on Sugi et al. (1990); the planetary boundary layer processes are parameterized following the Mellor-Yamada level 3 approach (Nakanishi and Niino 2006) and the land surface scheme are parameterized following Beljaars and Holtlag (1991).

We focus our model evaluation on precipitation given its critical importance for assessing climate change impacts on ecosystems and society (Fosser et al. 2015). The precipitation validation data are taken from WorldClim database (Hijmans et al. 2005; <http://www.worldclim.org>; see Sect. S2). Although the climatological period of the model (1986–2005) and observations (1950–2000) are non-overlapping, for the purposes of assessing model performance with respect to annual precipitation and the seasonal cycle, they are still comparable owing to the relatively long period over which they are computed (Dai 2006; Selman and Misra 2015). We also note that WorldClim represents a statistical interpolation of gauge-based observations and as such is also subject to its own errors and biases.

3 Results

3.1 (a) Validation of twentieth-century simulation

The climatological seasonal cycle of the observed rainfall, including its annual mean, clearly shows (Fig. 2a–e) that the north-south gradient of precipitation is strongly related with the orography of the region. This spatial gradient is most prominent in the summer months (JJA;

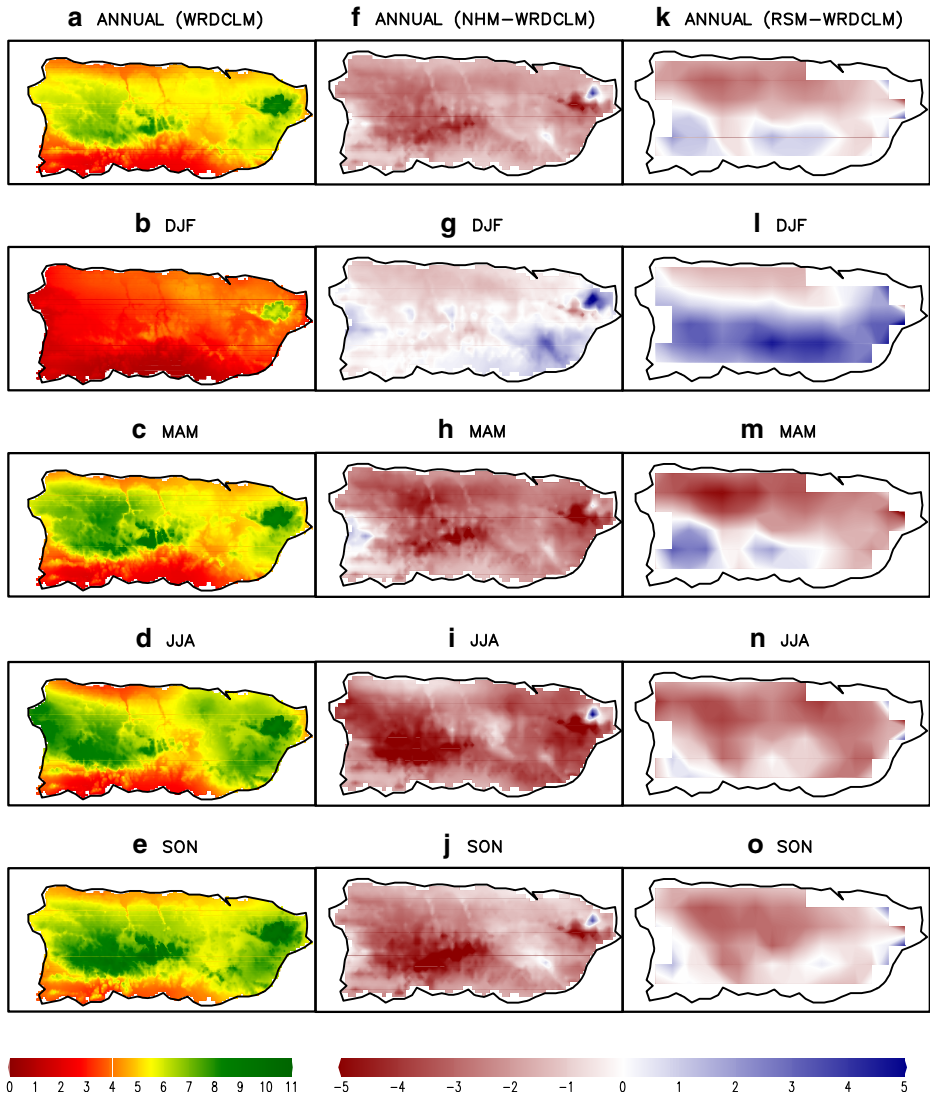


Fig. 2 The observed (WorldClim; Hijijmans et al. 2005) climatological (1950–2000) seasonal cycle of rainfall (mm day^{-1}) including **a** annual mean, **b** December–January–February (DJF), **c** March–April–May (MAM), **d** June–July–August (JJA), and **e** September–October–November (SON). The corresponding systematic errors (mm day^{-1}) of NHM (based on climatology over period of 1986–2005) for **f** annual mean, **g** DJF, **h** MAM, **i** JJA, and **j** SON and RSM for **k** annual mean, **l** DJF, **m** MAM, **n** JJA, and **o** SON

Fig. 2d) and weakest in the winter season (DJF; Fig. 2b). In the winter, the entire island is significantly drier than during the rest of the year. There is also a local maximum of observed precipitation sustained throughout the year in the northeastern part of island where the Luquillo Mountains are located. The corresponding systematic errors (Fig. 2f–j) and the seasonal cycle of the NHM (Fig. 3a–e) indicate that the seasonal cycle is qualitatively maintained, although with a significant dry bias. The NHM exhibits a dry (wet) bias in northern (eastern) part of the island in the winter season (Fig. 2g). But there is overall dry bias over the island in the spring, summer, and fall seasons (Fig. 2h, i and j), which gets reflected in the annual mean (Fig. 2f). It may, however, be noted that the NHM is able to simulate the local maximum of rainfall throughout the year near Sierra de Luquillo (Fig. 3a–e). In comparison, RSM exhibits a similar precipitation bias pattern to the NHM (Fig. 2k–o) but with a severe wet bias in the southern part of the island in DJF (Fig. 2l) and MAM (Fig. 2m) seasons. We note however that part of this dry bias in NHM and RSM is contributed by the CCSM4 forcing. Kozar and Misra (2013) point to a systematic cold bias of SST in all CMIP5 models over the Caribbean Sea region that is used to force RSM and NHM. Ryu and Hayhoe (2013) also point to a similar dry precipitation bias over the region in the twentieth-century simulations of CMIP5 including CCSM4.

The impact of nesting NHM within the RSM simulation is, however, evident from comparing the corresponding systematic errors in the seasonal cycle from RSM (Fig. 2l–o). Annual mean precipitation as simulated by RSM (Figs. 2k and 3k) shows biases characterized by a wetter southern and a drier northern Puerto Rico, implying a north–south gradient contrary to observations. This bias in RSM is not surprising given the relatively coarse resolution of the model to resolve the local orography (Fig. 1c). The wet bias over the entire island in DJF is greatly exacerbated in RSM (Fig. 2l). Similarly, the severe wet bias in the southern part of the island in RSM persists albeit weakly in the spring (Fig. 2m). This spring season wet bias is significantly reduced in NHM (Fig. 2h). However, the dry bias north of the Cordillera Central displayed in spring (Fig. 2m) and summer (Fig. 2n) by RSM is comparable to the corresponding NHM bias (Fig. 2h and i), and the dry bias in the western part of the island displayed by NHM in Fig. 2i and j is moderately reduced in RSM (Fig. 2n and o).

3.2 (b) Projected change in rainfall seasonality in mid-twenty-first century

Despite these biases in the NHM, it is notable that the overall drying trend in the region (Fig. 3f–j; especially during the wet season in JJA (Fig. 3i)) is consistent across CCSM4, RSM, and NHM (Fig. SF1), which indicates that there is a large-scale contribution to this trend. It should however be noted that the CCSM4 simulation does not resolve the island of Puerto Rico (Fig. 1d). The local spatial gradients of rainfall owing to the orography are exclusively resolved at the NHM spatial resolutions (Fig. SF1). It may be noted that the statistical significance of this dry trend over Puerto Rico is observed across all three models (Figs. SF1 and 3). This suggests that the climate change signal in summer rainfall is sustained in NHM despite the increase in the internal variance of the climate system, pointing to the robustness of the result. The projected percentage change² in the seasonal mean rainfall in the mid-twenty-first century relative to the twentieth century simulation from the NHM is statistically significant (Fig. 3f–j). The percentage change of annual mean rainfall as projected by the NHM averaged over the island is –20 to –30% (with no indication of being wetter anywhere in the island; Fig. 3f). The NHM largely preserves the north–south precipitation gradient in the mid-twenty-first century over the island (Fig. SF2). In the mid-

² Is defined by $(\text{twenty-first-century mean} - \text{twentieth-century mean}) \times 100 / (\text{twentieth century-mean})$.

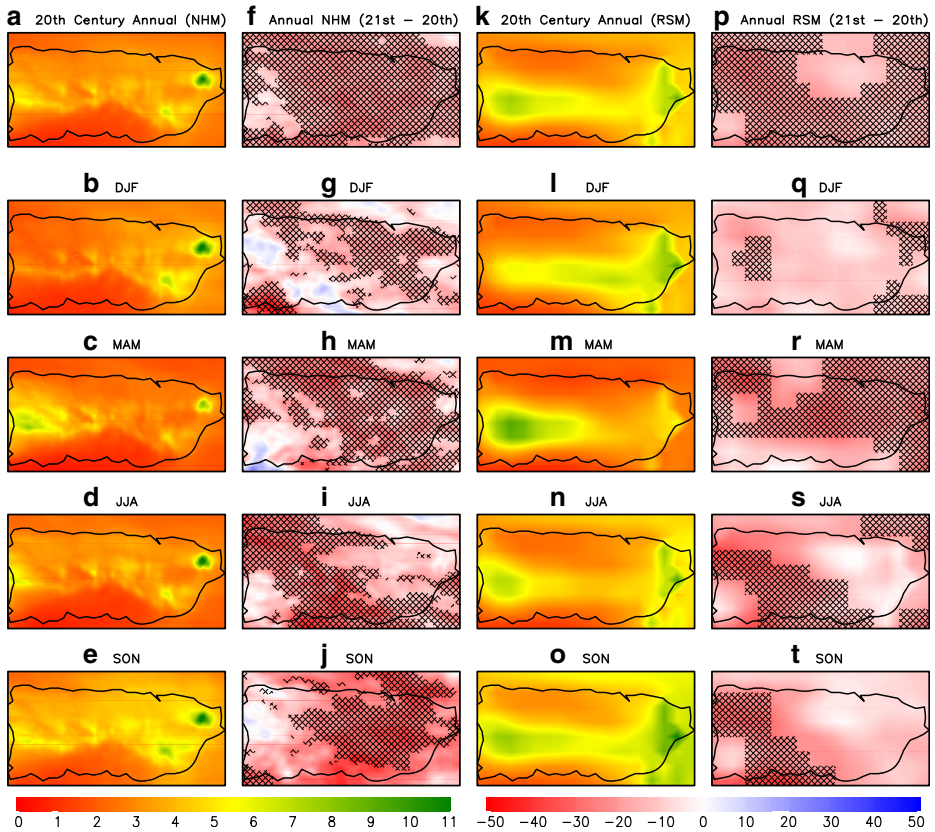


Fig. 3 The climatological seasonal cycle of rainfall (mm day^{-1}) from the twentieth century simulation (1986–2005) of the NHM including **a** annual mean, **b** DJF, **c** MAM, **d** JJA, and **e** SON. The corresponding (percent) change in the projected mid-twenty-first-century (2041–2060) climate from NHM for **f** annual mean, **g** DJF, **h** MAM, **i** JJA, and **j** SON. Similarly, the climatological seasonal cycle of rainfall from the twentieth-century simulation of RSM including **k** annual mean, **l** DJF, **m** MAM, **n** JJA, and **o** SON and corresponding projected change in mid-twenty-first-century climate from RSM for **p** annual mean, **q** DJF, **r** MAM, **s** JJA, and **t** SON. The color bar to the bottom left (right) represents shading interval for seasonal cycle (percent change) of rainfall. The statistically significant regions at 10% significance level according to two-tailed t test is hashed in the difference plots

twenty-first century, NHM indicates that there is a slight diminishment of the gradient in the rainfall between the north and south of Cordillera Central in all seasons relative to the late twentieth-century simulation (Fig. SF2). This is because the northern part of the island dries out slightly more than the southern part of the island in the mid-twenty-first century. This diminishment is weakest during the fall season (Fig. SF2d) and strongest in the spring season (Fig. SF2b). It may be noted that the NHM finds the drying in the southern part of the island (south of the peak of Cordillera Central) in DJF to be statistically insignificant (Fig. SF2a). However, Fig. SF2 reconfirms the erroneous meridional gradient of rainfall simulated by RSM over Puerto Rico, which is clearly the manifestation of the misrepresentation of the Cordillera Central in the RSM (Fig. 1b). This highlights yet again the importance of dynamic downscaling to high spatial resolutions for discerning climate change signal at such local scales for Puerto Rico.

We also analyzed the results by examining the changes to the seasonal cycle in area averaged precipitation in the northwest (NW), northeast (NE), southwest (SW), and southeast (SE) parts of

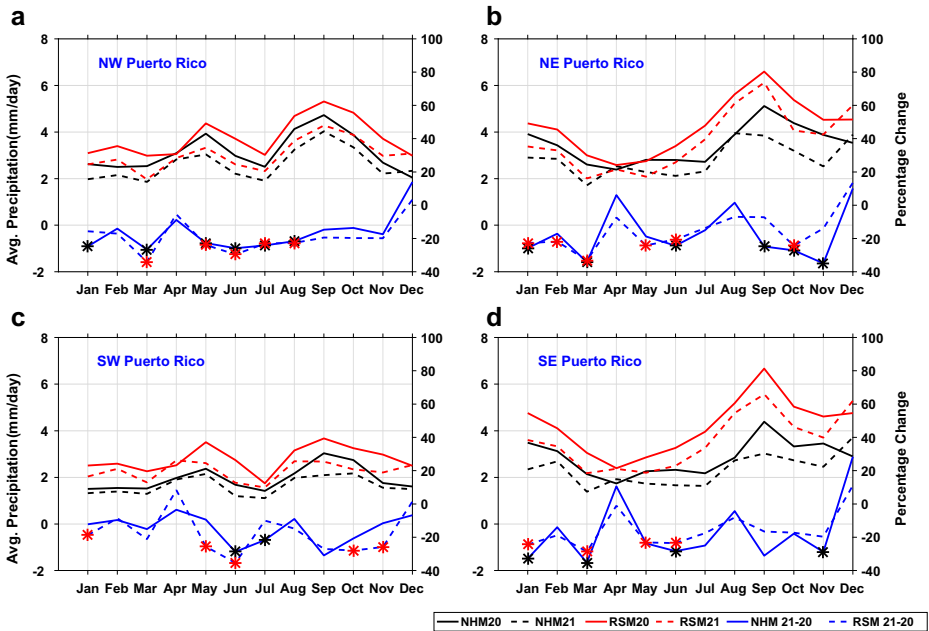


Fig. 4 The climatological seasonal cycle of rainfall averaged over the **a** NW, **b** NE, **c** SW, and **d** SE parts of Puerto Rico from the twentieth- and twenty-first-century simulations from NHM and RSM. The statistically significant values at 10% significance level using a two tailed *t* test for the projected change are shown with black and red asterisk marks for the NHM and RSM projected change, respectively

the island (Fig. 4). These four sectors are based on the latitude and longitude lines passing through the geographical center of the island (see Fig. 1b and c). In these figures, a temporary dry period referred to as the mid-summer drought (MSD), is quite apparent in the NW (Fig. 4a) and SW (Fig. 4c) parts of the island, with a dual peak of rainfall in May and in September and a relative minimum in July. The rainfall at MSD in the western portion of the island is comparable to drier seasons, and the amplitude of this seasonal cycle as measured by the climatological values of the rainfall peaks and nadir (of the MSD) in both centuries is weaker in the NHM relative to the RSM (Table ST3). Furthermore, in the northwest and southwest regions of Puerto Rico, both models show a smaller decrease of rainfall in July but a relatively larger decrease during the seasonal maximum, especially in May in the mid-twenty-first century relative to the late twentieth-century simulation (Table ST3). This leads to the conclusion that the model projects a diminished MSD phenomenon in a future climate over the western part of Puerto Rico owing to smaller rainfall differences between the drought period and the period of rainfall maximum surrounding the MSD. In addition, NHM displays a comparable diminishment of fall season rainfall (as in the summer season) in the mid-twenty-first century relative to late twentieth century in the SW (Fig. 4c) of the island. On the other hand, in the eastern half of the island, the rainfall peaks in early fall season, which is sustained in the mid-twenty-first century, albeit more weakly (Fig. 4b and d). In fact, the largest reductions of rainfall in the mid-twenty-first century occur in the northeastern part of the island in the fall season in NHM followed by the drying in late-spring and early-summer season (Fig. 4b).

3.3 (c) Projected change in rainfall at sub-daily and daily timescales in the mid-twenty-first century

In Fig. 5, we show the change in the frequency of occurrence of hourly rainfall rates (that correspond between 98.776 and 99.999 percentile) for the four sub-domains over Puerto Rico from the NHM simulations between the late twentieth- and mid-twenty-first-century simulations. For this portion of the analysis, we have avoided an attempt to analyze individual storm events with tropical cyclone characteristics due to: (1) the restricted domain of NHM which limits the ability to resolve the translation of tropical cyclones into the vicinity of and across the island, (2) the persistent bias in the model simulations, and (3) the relatively infrequent incidence of land falling tropical cyclones (five tropical cyclone landfalls in 1986–2005 period). While such an analysis may be informative for evaluating the potential reasons for changing precipitation extremes, it would not affect the analysis of that change in and of itself.

Except for the winter season in the NE (Fig. 5a) and SE (Fig. 5c) regions, we find that for each sub-domain and season combination, the frequency of the most extreme hourly rainfall

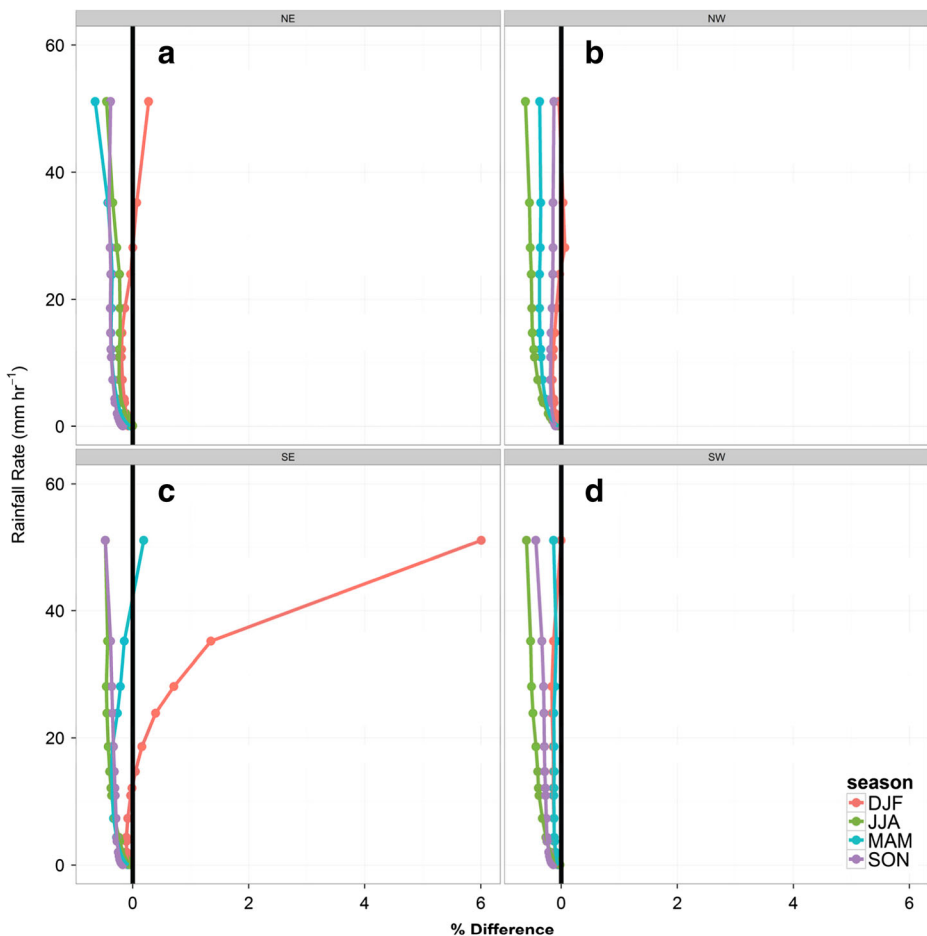


Fig. 5 The (percent) change in frequency of hourly rain rates between late twentieth- and mid-twenty-first-century simulations from NHM for rain rates over **a** NE, **b** NW, **c** SE, and **d** SW parts of Puerto Rico

events is slightly reduced in the mid-twenty-first century relative to the late twentieth-century simulation (see Sect. S3 and Fig. SF3). This reduction is most prominent during the summer season (JJA) over NW and SW followed by reductions in the spring season (MAM) over NE and NW part of the island. Interestingly, the simulations indicate that NE and SE parts of the island experience an unusual increase in the frequency of extreme hourly rain rate events in the mid-twenty-first century in the winter (DJF) season (Figs. 4c and SF3a and c). The reason for this increase is not immediately apparent and will require further investigation.

Similarly, the changing frequencies of daily rain rates between the late twentieth- and mid-twenty-first-century simulations over the various sub-domains of Puerto Rico are shown in Fig. SF4. Here, we find that the NE Puerto Rico sub-region displays a slight increase in the frequency of rain rates over a wide portion of the distribution in a future climate except in the spring season. In all other sub-domains and seasons, there is a reduction in the frequency of daily rain rates with additional exceptions over the western part of the island (NW and SW) and SE regions in the MAM and DJF seasons, respectively (Fig. SF4). The RSM also shows similar changes to the hourly and daily rain rates over all four regions as NHM in the projected mid-twenty-first century climate (not shown).

This pervasive drying of the projected climate over Puerto Rico is found across all three model configurations (CCSM4, RSM, and NHM; Fig. SF1). These results are consistent with predictions that a warming climate in the (sub-tropical) regions that are within the margins of the active convective zones will experience drying through the proposed “upped ante” scheme or the “rich getting richer” mechanism (Neelin et al. 2003; Rauscher et al. 2011; Ryu and Hayhoe 2013). Such a mechanism is likely playing a role in the drying seen in all three model simulations of this study. But at the more local scale of NHM, we find that the weakening trade winds (Fig. 6) and the large-scale increased subsidence forced by the neighboring active convective zone of the intertropical convergence zone in a future climate (Rauscher et al. 2011) result in reduced orographic lift or omega at 500 hPa near the mountains (Fig. SF5). In addition, the increased atmospheric stability of the future climate (not shown) from the warming of the tropospheric column (Fig. 6) results in reduced precipitation over the island despite an increase in the total precipitable water of the atmospheric column (Fig. SF6).

4 Discussion and conclusions

With a densely inhabited population of 3.4 million people, Puerto Rico is vulnerable to climate change. Earlier studies have suggested an overall reduction in rainfall because of the warming of the surrounding SST and associated deceleration of the easterly trade winds. In this study, we have downscaled a GCM operating at an approximately 150-km grid interval to an unprecedented 2-km grid interval, providing sufficient resolution to resolve local orographic features and convection. The local orography includes mountain ranges (Cordillera Central and the Luquillo Mountains), which although not highly elevated, force a steep precipitation gradient that results in a commensurate diversity of ecosystems and habitats that are sensitive to changes in climate. The results of this study indicate that the dominant north-south gradient of rainfall enforced by the Cordillera Central and the local rainfall maxima in the northeastern part of the island around the windward side of the Luquillo Mountains would diminish by the mid-twenty-first century relative to the current climate under the RCP8.5 emission scenario.

The high spatial resolution of the NHM is deemed important to discern the orographically forced meridional rainfall gradient between the northern and southern parts of the island owing

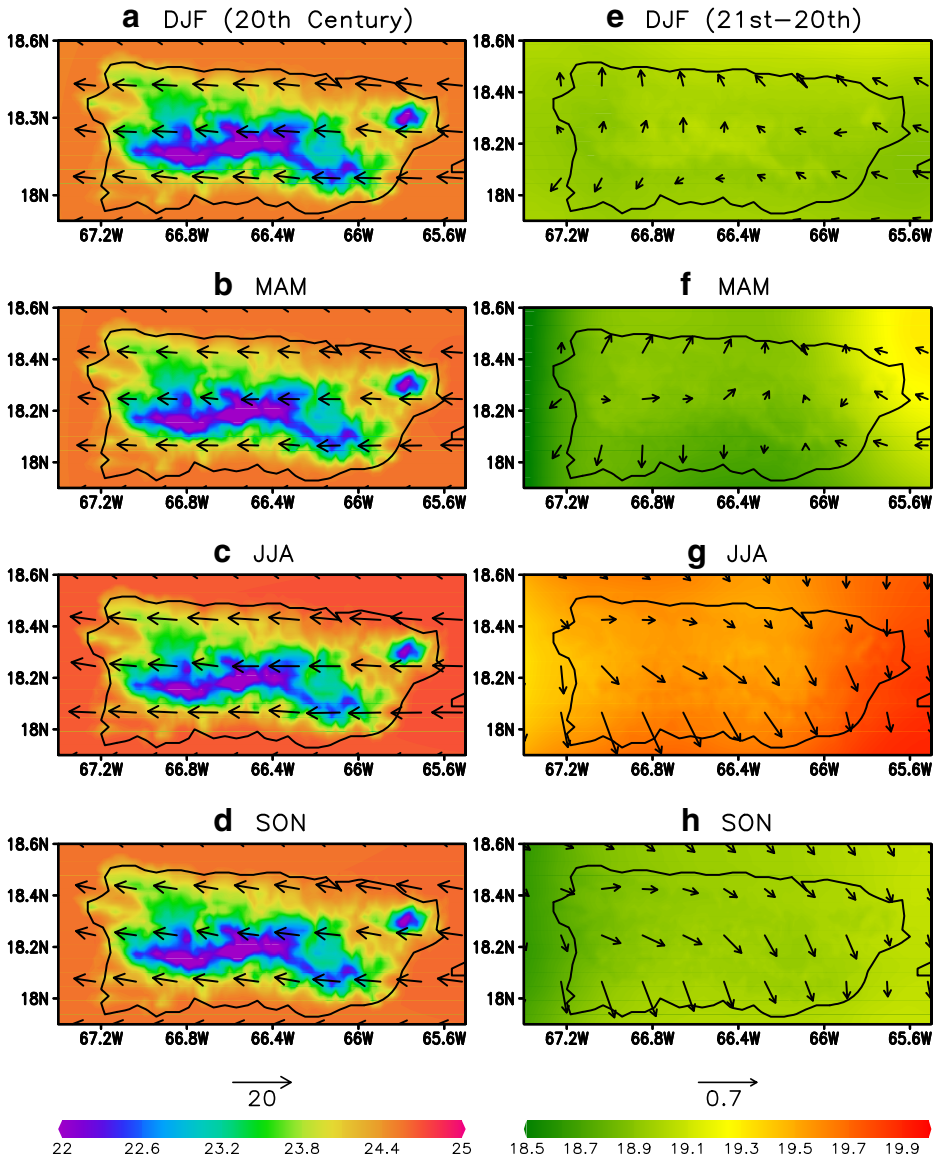


Fig. 6 The tropospheric temperature (shaded; $\text{K kg m}^{-2} \times 10^5$) and 850-hPa winds (m s^{-1}) from the twentieth century simulation of NHM for **a** DJF, **b** MAM, **c** JJA, and **d** SON. The corresponding projected change (for tropospheric temperature units are in $\text{K kg m}^{-2} \times 10^3$; shaded) in the mid-twenty-first century relative to the late twentieth-century simulations of the NHM for **e** DJF, **f** MAM, **g** JJA, and **h** SON seasons. The statistically significant regions at 10% significance level according to two-tailed t test are shaded in the difference plots

to its resolution of the topography and convective-permitting scales. The results of climate change experiments become less meaningful when such local gradients forced by local land surface features are not simulated. We find that the local manifestation of the global climate change signal over the island is characterized by an overall diminishment of the precipitation over the island that also results in the reduction of the north-south precipitation gradient. The

MSD phenomenon in the northwestern part of the island also becomes less prominent in a future climate with this overall drying over the island. This signal is sustained even when the model (NHM) resolves more internal variance proving the robustness of the result.

This drying climate change signal over Puerto Rico is simulated in the presence of a warmer and a more stable atmospheric column that paradoxically also contains more water vapor. This warming and moistening of the terrestrial atmosphere over Puerto Rico would normally lead one to predict an increase in extreme rainfall events (Wuebbles et al. 2014; Trenberth et al. 2015). But this study finds that rainfall extremes at sub-daily and daily time scales become less frequent in the mid-twenty-first century relative to present conditions across most seasons and sub-regions of the island. The increasing stability of the atmospheric column due to the warming, combined with a reduction in orographic lift caused by reduced trade winds, and increased subsidence over the subtropical regions from comparatively more active convective zones (Neelin et al. 2003; Rauscher et al. 2011), results in an overall drying of the island and a pervasive reduction in extreme rainfall occurrence.

Importantly, these results are subject to the caveat that this experiment is based on the downscaling of a single GCM. Additional integrations with multiple GCMs and a second NHM are currently underway. But the conclusions of the study are in agreement with prior downscaling studies that included multi-model GCM ensembles (Campbell et al. 2011; Hayhoe 2013).

Acknowledgements We would like to thank Tracy Ippolito for reviewing our manuscript for editorial corrections.

Funding information This work was supported by grants from NOAA (NA12OAR4310078, NA10OAR4320143, NA11OAR4310110) and USGS G13AC00408. The supercomputing facility provided by XSEDE under grant number ATM10010 was used to complete the model integrations used in this study.

References

- Andrews T et al (2012) Forcing, feedbacks, and climate sensitivity in CMIP5 coupled atmosphere-ocean climate models. *Geophys Res Lett* 39:L09712. <https://doi.org/10.1029/2012GL051607>
- Beljaars ACM, Holtslag AAM (1991) Flux parameterization over land surfaces for atmospheric models. *J Appl Meteorol* 30:327–341
- Bellenger H et al (2014) ENSO representation in climate models: from CMIP3 to CMIP5. *Climate Dynamics* 42(7–8):1999–2018
- Bitz CM et al (2012) Climate sensitivity of the Community Climate System Model, version 4. *J Clim* 25:3053–3070
- Borga M et al (2011) Flash flood forecasting, warning, and risk management: the HYDRATE project. *Env Res Lett* 14:834–844
- Bowden JH et al (2012) Examining interior grid nudging techniques using two-way nesting in the WRF model for regional climate modeling. *J Clim* 25:2805–2823
- Bowden JH, Nolte CG, Otte TL (2013) Simulating the impact of the large-scale circulation on the 2-m temperature and precipitation climatology. *Clim Dyn* 40:1903–1920
- Campbell JD et al (2011) Future climate of the Caribbean from a regional climate model. *Int J Climatol* 31:1866–1878
- Cantet P, et al. (2014) The importance of using a high resolution model to study the climate change on small islands: the Lesser Antilles case. *Tellus A*, 66(0)
- Chan SC, Misra V, Smith H (2011) A modeling study of the interaction between the Atlantic warm pool, the tropical Atlantic easterlies, and the Lesser Antilles. *J Geophys Res* 116:D00Q02. <https://doi.org/10.1029/2010jd015260>
- Comarazamy DE, Gonzalez JE (2011) Regional long-term climate change (1950–2000) in the mid-tropical Atlantic and its impacts on the hydrological cycle of Puerto Rico. *J Geophys Res* 116:D00Q05. <https://doi.org/10.1029/2010JD015414>

- Dai A (2006) Precipitation characteristics in eighteen coupled climate models. *J Clim* 19:4605–4630
- DiNapoli S, Misra V (2012) Reconstructing the 20th century high-resolution climate of the southeastern United States. *J Geophys Res* 117:D19113. <https://doi.org/10.1029/2012JD018303>
- Fosser G, Khodayar S, Berg P (2015) Benefit of convection permitting climate model simulations in the representation of convective precipitation. *Clim Dyn* 44:45–60
- Gent PR et al (2011) The Community Climate System Model version 4. *J Clim* 24:4973–4991
- Gonzalez G, Luce MM (2013) Woody debris characterization along an elevation gradient in northeastern Puerto Rico. *Ecol Bull* 54:181–194
- Haerter JO, Berg P (2009) Unexpected rise in extreme precipitation caused by a shift in rain type? *Nat Geosci* 2:372–373
- Hall TC et al (2013) Future climate of the Caribbean from super-high resolution atmospheric general circulation model. *Theor Appl Climatol* 113(2013):271
- Hawkins E, Sutton R (2009) The potential to narrow uncertainty in regional climate predictions. *Bull Amer Soc* 90:1095–1107
- Hayhoe K (2013) Quantifying key drivers of climate variability and change for Puerto Rico and the Caribbean. Final report 1 241 p. Agreement No.: G10AC00582
- Henareh KA et al (2016) Climate change implications for tropical islands: interpolating and interpreting statistically downscaled GCM projections for management and planning. *J Appl Meteorol Climatol* 55:265–282
- Hijmans RJ et al (2005) Very high resolution interpolated climate surfaces for global land areas. *Int J Climatol* 25:1965–1978
- Ikawa M, Saito K (1991) Description of a non-hydrostatic model developed at the Forecast Research Department of the MRI. *MRI Tech Rep* 28:238
- Jury MR, Chiao S (2013) Leese boundary layer confluence and afternoon thunderstorms over Mayaguez, Puerto Rico. *Mon. Wea. Rev.* 52:439–454
- Kanamaru H, Kanamitsu M (2007) Scale-selective bias correction in a downscaling of global analysis using a regional model. *Mon Weather Rev* 135:334–350
- Kanamitsu M et al (2010) Errors of interannual variability and multi-decadal trend in dynamical regional climate downscaling and its corrections. *J Geophys Res* 115:D17115
- Kendon EJ et al (2014) Heavier summer downpours with climate change revealed by weather forecast resolution model. *Nat Clim Chang* 4:570–576
- Kozar ME, Misra V (2013) Evaluation of twentieth-century Atlantic Warm Pool simulations in historical CMIP5 runs. *Clim Dyn* 10:2375–2391
- Lenderink G, vanMeijgaard E (2008) Increase in hourly precipitation extremes beyond expectations from temperature changes. *Nat Geosci* 1:511–514
- Min SK et al (2011) Human contribution to more-intense precipitation extremes. *Nature* 470:376–379
- Misra V (2006) Addressing the issue of systematic errors in a regional climate model. *J Clim* 20:801–818
- Misra V, DiNapoli S, Bastola S (2012) Dynamic downscaling of the 20th century reanalysis over the southeastern United States *Regional Environmental Change* 13:15–23
- Nakanishi M, Niino H (2006) An improved Mellor-Yamada level-3 model: its numerical stability and application to a regional prediction of advection fog. *Bound-Layer Meteor* 119:397–407
- Neelin J, Chou C, Su H (2003) Tropical drought regions in global warming and El-Nino teleconnections. *Geophys Res Lett* 30(24):2275
- Palmer TN (2001) A nonlinear dynamical perspective on model error: a proposal for nonlocal stochastic-dynamic parameterization in weather and climate prediction models. *QJRMS* 127:279–304
- Peters GP et al (2013) The challenge to keep global warming below 2 °C. *Nat Clim Chang* 3(1):4–6
- Rauscher S, Kucharski A, Enfield D (2011) The role of regional SST warming variations in the drying of Meso-America in future climate projections. *J Clim* 24:2003–2016
- Riahi K et al (2011) RCP8.5—a scenario of comparatively high greenhouse gas emissions. *Clim Chang* 109:33–57
- Ryu J-H, Hayhoe K (2013) Understanding the sources of Caribbean precipitation biases in CMIP3 and CMIP5 simulations. *Clim Dyn* 42:3233–3252
- Saito K et al (2001) A global version of the Meteorological Research Institute/Numerical Prediction Division non-hydrostatic model. *CAS/JSC WGNE Res Activ Atmos Oceanic Modell* 31:6.20–6.21
- Saito K et al (2006) The operational JMA non-hydrostatic mesoscale model. *MonWea Rev* 134:1266–1298
- Selman C, Misra V (2015) Simulating diurnal variations over the southeastern United States. *J Geophys Res* 120:180–198
- Stefanova L et al (2012) A proxy for high resolution regional reanalysis for the southeast United States: assessment of precipitation variability. *Clim Dyn* 38:2449–2446

- Sugi M et al (1990) Description and performance of the JMA operational global spectral model (JMAGSM88). *Geophys Mag* 43:105–130
- Taylor KE, Stouffer RJ, Meehl GA (2012) An overview of CMIP5 and the experiment design. *Bull Am Meteorol Soc* 93:485–498
- Trenberth KE, Fasullo JT, Shepherd TG (2015) Attribution of climate extreme events. *Nat Clim Chang* 5:725–730
- Von Storch H, Langenberg H, Feser F (2000) A spectral nudging technique for dynamical downscaling purposes. *Mon Wea Rev* 128:3664–3673
- Waide RB et al (2013) Climate variability at multiple spatial and temporal scales in the Luquillo Mountain, Puerto Rico. *Ecol Bull* 54:21–41
- Wooten A et al (2016) The sensitivity of WRF downscaled precipitation in Puerto Rico to cumulus parameterization and interior grid nudging. *J Appl Meteorol Climatol*. <https://doi.org/10.1175/JAMC-D-16-0121.1>
- Wuebbles DJ et al (2014) CMIP5 climate model analyses: climate extremes in the United States. *Bullet Am Meteorol Soc*. <https://doi.org/10.1175/BAMS-D-12-00172.1>